AD-A050 637 AEROSPACE CORP EL SEGUNDO CALIF IVAN A GETTING LABS F/G 4/1
SIGNATURE OF A PARALLEL ELECTRIC FIELD IN ION AND ELECTRON DIST--ETC(U)
FEB 78 D R CROLEY, P F MIZERA, J F FENNELL F04701-77-C-0078
UNCLASSIFIED TR-0078(3960-5)-5 SAMSO-TR-78-38 NL

| OF |
AD
A050637

END
DATE
FILMED
4 -78
DDC

REPORT SAMSO-TR-78-38

Signature of a Parallel Electric Field in Ion and Electron Distributions in Velocity Space

D. R. CROLEY, Jr., P. F. MIZERA, and J. F. FENNELL
Space Sciences Laboratory
The Ivan A. Getting Laboratories
The Aerospace Corporation
El Segundo, Calif. 90245

6 February 1978

Interim Report

Prepared for

SPACE AND MISSILE SYSTEMS ORGANIZATION
AIR FORCE SYSTEMS COMMAND
Los Angeles Air Force Station
P.O. Box 92960, Worldway Postal Center
Los Angeles, Calif. 90009

This interim report was submitted by The Aerospace Corporation, El Segundo, CA 90245, under Contract No. F04701-77-C-0078 with the Space and Missile Systems Organization, Deputy for Advanced Space Programs, P.O. Box 92960, Worldway Postal Center, Los Angeles, CA 90009. It was reviewed and approved for The Aerospace Corporation by G. A. Paulikas, Director, Space Sciences Laboratory. Lieutenant Dara Batki, SAMSO/YCPT, was the project officer for Advanced Space Programs.

This report has been reviewed by the Information Office (OI) and is releasable to the National Technical Information Service (NTIS). At NTIS, it will be available to the general public, including foreign nations.

This technical report has been reviewed and is approved for publication. Publication of this report does not constitute Air Force approval of the report's findings or conclusions. It is published only for the exchange and stimulation of ideas.

Dara Batki
Dara Batki, Lt, USAF
Project Officer

Robert W. Lindemuth
Robert W. Lindemuth, Lt Col, USAF
Chief, Technology Plans Division

FOR THE COMMANDER

Leonard E. Baltzell
LEONARD E. BALTZELL, Col, USAF
Asst. Deputy for Advanced
Space Programs

UNCLASSIFIED

SECURITY CLASSIFICATION OF THIS PAGE (When Data Entered)

REPORT DOCUMENTATION PAGE		READ INSTRUCTIONS BEFORE COMPLETING FORM
1. REPORT NUMBER SAMSO-TR-78-38	2. GOVT ACCESSION NO.	3. RECIPIENT'S CATALOG NUMBER
4. TITLE (and Subtitle) SIGNATURE OF A PARALLEL ELECTRIC FIELD IN ION AND ELECTRON DISTRIBUTIONS IN VELOCITY SPACE.		5. TYPE OF REPORT & PERIOD COVERED Interim rept.
		6. PERFORMING ORG. REPORT NUMBER TR-0078(3960-05)-5
7. AUTHOR(s) Donald R. Croley, Jr., Paul F. Mizera Joseph F. Fennell		8. CONTRACT OR GRANT NUMBER(s) F04701-77-C-0078
9. PERFORMING ORGANIZATION NAME AND ADDRESS The Aerospace Corporation El Segundo, Calif. 90245		10. PROGRAM ELEMENT, PROJECT, TASK AREA & WORK UNIT NUMBERS
11. CONTROLLING OFFICE NAME AND ADDRESS Space and Missile Systems Organization Air Force Systems Command Los Angeles, Calif. 90009		12. REPORT DATE 6 Feb 78 13. NUMBER OF PAGES 17 (12) 21p.
14. MONITORING AGENCY NAME & ADDRESS(if different from Controlling Office)		15. SECURITY CLASS. (of this report) Unclassified 15a. DECLASSIFICATION/DOWNGRADING SCHEDULE

16. DISTRIBUTION STATEMENT (of this Report)

Approved for public release; distribution unlimited

17. DISTRIBUTION STATEMENT (of the abstract entered in Block 20, if different from Report)

18. SUPPLEMENTARY NOTES

To be published in Journal of Geophysical Research

19. KEY WORDS (Continue on reverse side if necessary and identify by block number)

Phase Space Diagrams
Electrostatic Acceleration

20. ABSTRACT (Continue on reverse side if necessary and identify by block number)

Charged particle data taken by the S3-3 satellite, reported by Mizera and Fennell (1977), are presented as contours of the velocity distribution function on a velocity-space diagram. This report focuses on the analytical technique used to interpret the particle data. Details of features exhibited by the electron and ion data in the velocity space representations are discussed in terms of a simple electrostatic acceleration model. The observed particle populations are separated in velocity-space by recognizable demarcations calculated from the conservation laws in accordance with Liouville's theorem.

DD FORM (FACSIMILE) 1473

UNCLASSIFIED

SECURITY CLASSIFICATION OF THIS PAGE (When Data Entered)

409 944

PREFACE

We wish to thank the large number of people at The Aerospace Corporation and the Air Force who made the S3-3 program successful. We would like especially to thank Drs. Y. T. Chiu and Michael Schulz for the many helpful theoretical discussions, Dr. H. H. Hilton for the ephemeris and attitude calculations, and Ms. Vera Bledsoe and Ms. Gwen Boyd for their assistance in performing the calculations.

CONTENTS

FIGURES

INTRODUCTION

Recent charged particle data acquired by the S3-3 satellite, with good spatial and temporal resolution, have been reported (Mizera and Fennell, 1977) for an auroral event on August 12, 1976, in the northern auroral zone giving convincing evidence of the existence of a parallel electric field extending from above the satellite (7330 km) down to the ionosphere. The purpose of this report is to elaborate on the analysis which brings into focus the electric field signature seen in the electron and ion distribution functions.

The features of the particle population can be viewed completely when a full satellite spin period (approximately 19 seconds) of data is displayed in a velocity-space representation as contours of constant velocity distribution function

$$f(v) = m^2 J/2E \quad (\sec^3/km^6) \,, \tag{1}$$

where J is the differential particle flux, E is the energy, m is the mass and v is the velocity of the ion or electron. Pitch angle distributions for each of the eight energy channels of the S3-3 electrostatic analyzers were used to determine the velocity distribution function at one-degree intervals. Each velocity distribution function was logarithmically interpolated to an arbitrary set of fixed values of f(v), which are logarithmically spaced. The set of energies corresponding to these fixed values of the distribution function at each one-degree increment of pitch angle were converted to parallel and perpendicular components of particle velocity with respect to the earth's magnetic field. This was done for both electrons and ions. Plotting the ($v_\parallel$, $v_\perp$) set of

points for a constant value of the distribution function at one-degree intervals produced a contour (Figure 1). In the northern hemisphere the $+v_{\parallel}$ axis corresponds to particles with 0^{o} pitch angle precipitating into the atmosphere. The $-v_{\parallel}$ axis corresponds to particles with 180^{o} pitch angle coming up the field line. Both the $+v_{\perp}$ axis and the $-v_{\perp}$ axis correspond to 90^{o} pitch angle particles. The time sequence of the acquired data begins at 0^{o} and proceeds counterclockwise to 360^{o}. Data from two consecutive half-spins are displayed on each plot.

The consequences of Liouville's theorem, applied to the dynamical trajectories of charged particles in phase space in the presence of a parallel electric field has been discussed by Whipple (1977) and by Chiu and Schulz (1978). For reasonably well-behaved electric potentials, expressed as functions of magnetic field intensity along a field line, the constants of motion of a charged particle can be used to interpret the data that have been organized in the velocity-space diagram. The presence of a potential drop along a magnetic field line restricts the access of particle populations to domains whose boundaries can be calculated from the constants of motion. For example, all of velocity-space at an arbitrary altitude below the satellite designated by the subscript ℓ transforms into a region bounded by a hyperbola at satellite altitudes. The equation of this hyperbola is

$$v_{\parallel}^{2} + [1 - (B_{\ell}/B)]\, v_{\perp}^{2} - (2q/m)\ |e|\ (V_{\ell} - V) = 0 \ , \qquad (2)$$

where B_{ℓ} is the magnitude of the earth's magnetic field at the altitude denoted by subscript ℓ (approximately 100 km for electrons), B is the earth's magnetic field at the

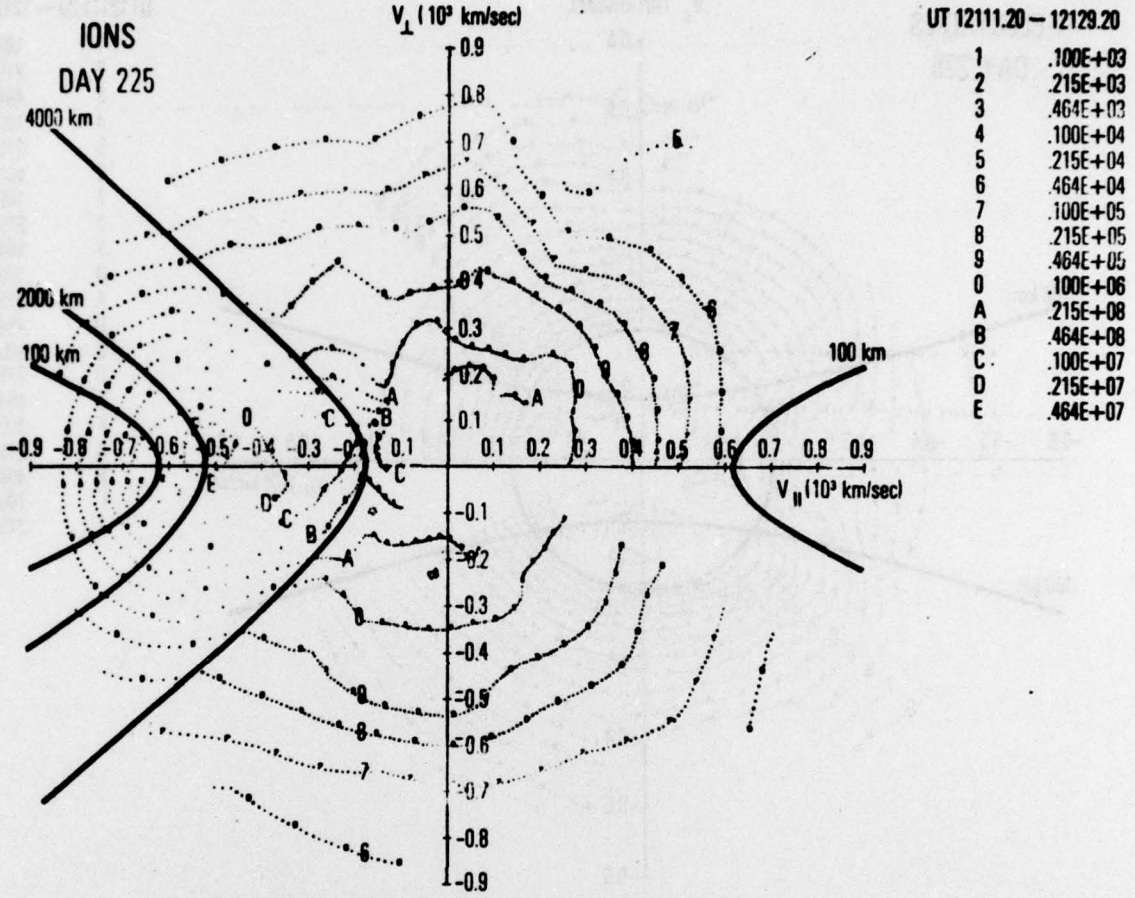

Figure 1a. Values of constant velocity-space distribution function $f(v) = m^2 J / 2E$ (sec^3-km^{-6}) are plotted for ions from data taken on August 12, 1976 between UT 12110 and UT 12129 (Mizera and Fennell, 1977). The solid curves are a family of hyperbolae calculated using parameters V_ℓ and B_ℓ in equation (2) representing altitudes of 100 km, 2000 km and 4000 km. The empty region surrounding the origin corresponds to energies below the threshold of the instrument. Other breaks in the contours are the result of data missing due to telemetry drop out or to particle fluxes which have fallen below the detection threshold of the instrument.

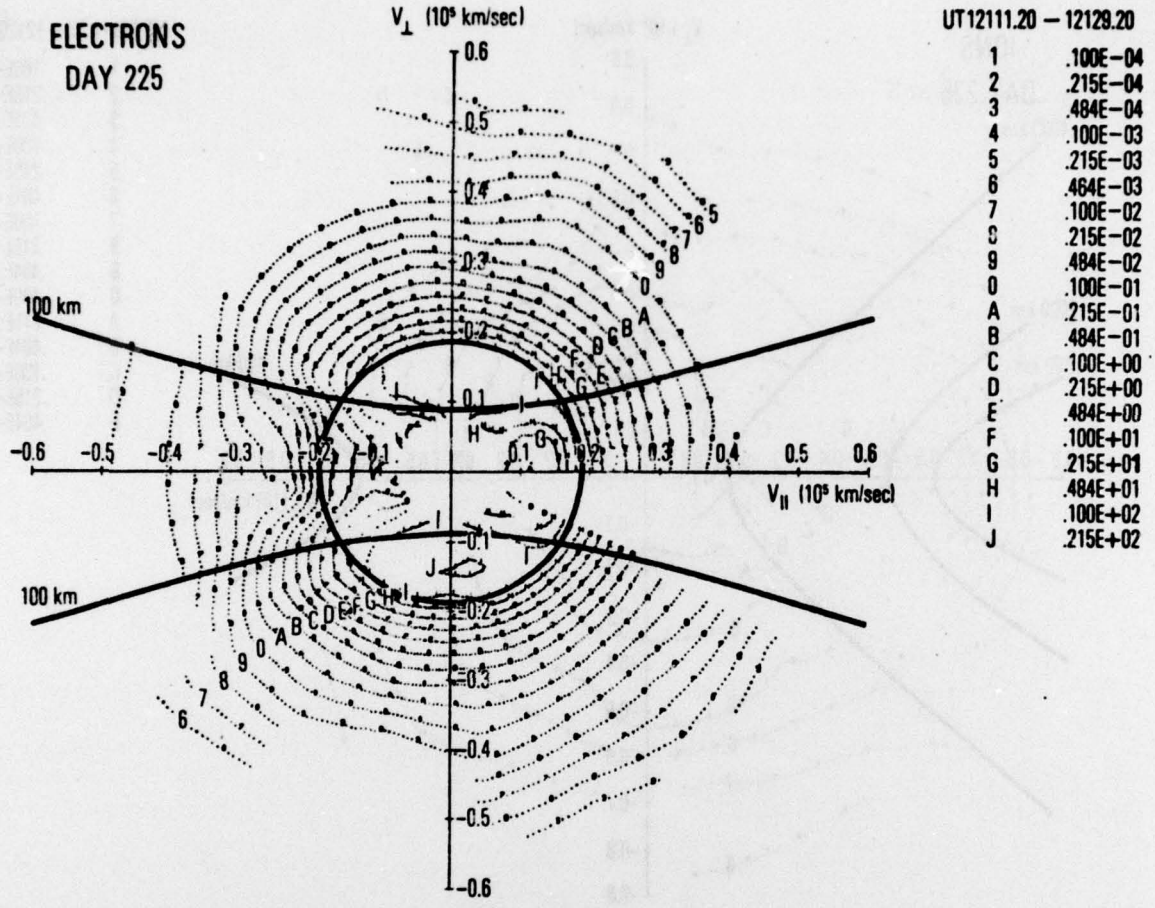

Figure 1b. Values of constant velocity-space distribution function are plotted for electrons corresponding to the ions shown in (a). The solid curves are the domain boundaries calculated from equations (2) and (3) by using values of the local potential V, determined by Mizera and Fennell (1977), and values of the parameters V_ℓ and B_ℓ representative of 100 km. The time sequence of the data begins along the $+v_{||}$ axis corresponding to particles traveling down the magnetic field line, and proceeds through pitch angles in a counter-clockwise direction. Two consecutive half spin periods are shown on the same plot.

satellite, V_ℓ is the potential at the altitude denoted by ℓ. V is the potential at the satellite, q is the sign of the charge and e is the electronic charge. Similarly the region in velocity-space which defines the trajectories of charged particles that are turned around by the electric field above the satellite is defined by the interior of an ellipse. The equation of this ellipse is

$$v_\parallel^2 + [1 - (B_o/B)] v_\perp^2 + (2q/m) |e| V = 0 , \qquad (3)$$

where B_o is the magnitude of the earth's magnetic field at the position on the magnetic field line above the satellite where the potential vanishes (arbitrarily taken here to be at the dipole field equator). Figure 2, taken from Chiu and Schulz (1978), shows schematically how the boundaries produced by equations (2) and (3) divide velocity-space into well defined regions. The regions in Figure 2 are labeled according to particle origin as allowed by access due to adiabatic motion. For the purpose of defining the nomenclature in Figure 2, the altitude denoted by the subscript ℓ has been chosen so that ideally the ionosphere is below and the magnetosphere is above.

The following discussion will serve to identify the various regions in velocity-space shown in Figure 2. The region labeled M in Figure 2a, which contains the origin (v = 0), is characterized by a positive ion population whose mirror points lie above the altitude denoted by ℓ, in the local hemisphere, and are magnetospheric in nature. In the $-v_\parallel$ direction, the region labeled I is characterized by ions coming from below the altitude denoted by ℓ, that is, from the ionosphere. The region along the $+v_\parallel$ axis labeled M, (I) is characterized by ions which are destined to mirror below the altitude denoted by ℓ. These

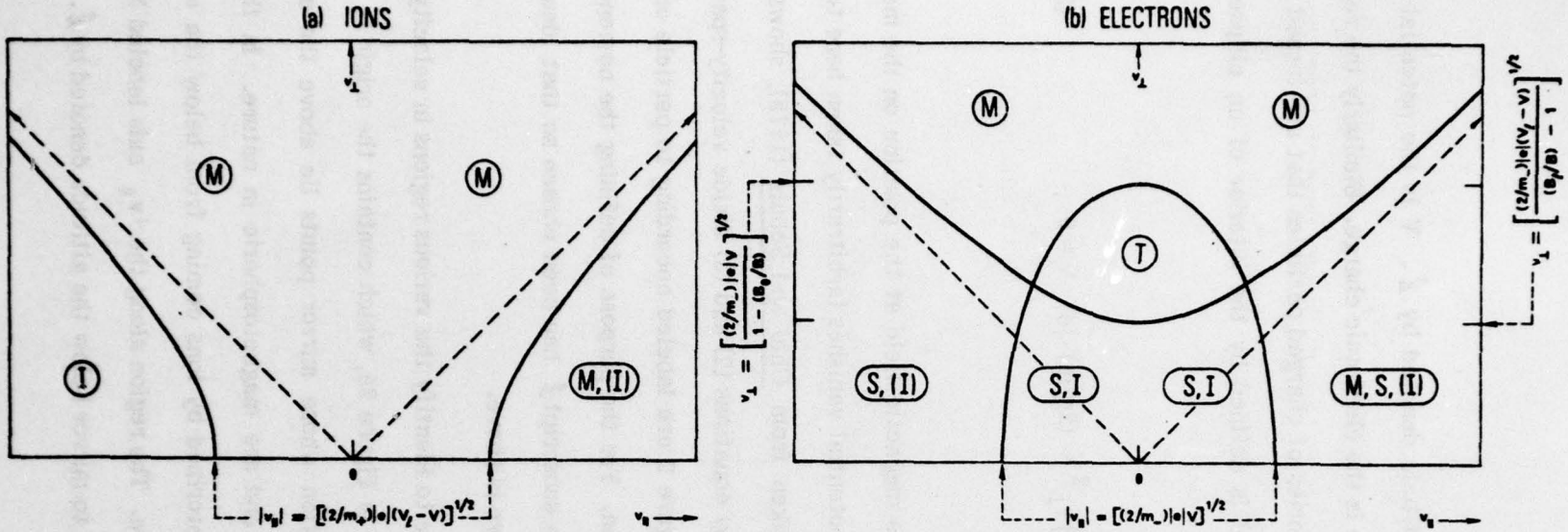

Figure 2. The regions of phase space occupied by the various particle populations are shown schematically for (a) ions and for (b) electrons (Chiu and Schulz, 1978). The solid curves are demarcations in phase space for the various populations of particles identified by labels in circles or in cartouches: M for particles of magnetospheric origin, S for backscattered electrons, and T for electrons trapped between mirror points that both lie on the same half of the field line. The electron labels I in parentheses indicate phase space regions occupied by electrons in the extreme tail of the cold ionospheric energy distribution. The dashed diagonal lines are the asymptotes $v_\parallel = \pm [(B_\ell/B) - 1]^{1/2} v_\perp$ of the hyperbolic phase space demarcations between $v_{\parallel\ell}^2 > 0$ and $v_{\parallel\ell}^2 < 0$. The dashed arrows relate the appropriate expression to the $v_\parallel$ and $v_\perp$ intercepts.

ions can be of magnetospheric origin or they may originate in the ionosphere of the conjugate hemisphere. The ions in regions M, (I) have an energy at the satellite sufficient to overcome the electric potential below. The ions in region I have all been accelerated by the electric field below. The $v_{\parallel}$ intercept shown in Figure 2a represents the minimum energy that ions in either of these regions can have.

The region above the hyperbola in Figure 2b is characterized by electrons whose mirror points lie above the altitude denoted by ℓ, whereas the whole region below the hyperbola is characterized by electrons with mirror points below the altitude denoted by ℓ. The ellipse is determined by the electric potential above the satellite. Electrons with velocities interior to the ellipse do not have sufficient energy to overcome the electric potential above the satellite and are turned around and accelerated back down the field line. The minimum energy an electron accelerated through the electric potential above the satellite can have is indicated by the $+v_{\parallel}$ intercept of the ellipse. The hyperbola and the ellipse divide electron velocity-space in Figure 2b into five basic regions. Region M is characterized by magnetospheric electrons which mirror above the ionosphere and which have been accelerated by the electric field above the satellite. The region denoted M, S, (I) along the $+v_{\parallel}$ axis is characterized by electrons which are destined to mirror in the ionosphere or atmosphere and which have been accelerated above the satellite. The region denoted S, (I) along the $-v_{\parallel}$ axis is characterized by electrons whose mirror points lie in the ionosphere below. This electron population is composed of high energy ionospheric electrons and high energy secondary electrons which are not confined by the parallel electric field. The region denoted by S, I has two parts. The region along the $-v_{\parallel}$ axis is characterized by secondary electrons or electrons of ionospheric origin whose

energy is not sufficient to escape the electric potential. These electrons, seen by the satellite as they travel up the magnetic field line, are turned around between the satellite and the equator. They appear in the measurements at the satellite in region S, I on the $+v_{\parallel}$ axis as they travel down the magnetic field line towards the ionosphere. Particular interest will be focused on the region denoted by T in Figure 2b, which is bounded by the ellipse and the hyperbola. Electrons whose trajectories occupy this region of velocity-space are trapped in the sense that they mirror magnetically above the ionosphere below the satellite and are turned around by the electric field above the satellite. Region T is a forbidden region in the sense that it cannot be populated by electrons from the magnetosphere or from the ionosphere by invoking a simple one-dimensional adiabatic theory. However, as the data will show, a significant electron population is found there. The expression for the $v_{\parallel}$ and $v_{\perp}$ intercepts of equations (2) and (3) are appropriately indicated on Figure 2.

OBSERVATIONS AND DISCUSSION

In the following discussion the data reported by Mizera and Fennell (1977), shown in Figure 1, will be examined in relation to boundaries determined by equations (2) and (3). It will be ascertained that particle populations manifested as contours of velocity distribution function are distinctly different across these boundaries. To establish these boundaries, values of B_ℓ , V_ℓ and B_o must be chosen. Some assumptions have to be made concerning the electric potential profile along the magnetic field line and the physical phenomena which violate the adiabatic character of the particle motion. Values assigned to these variables can be determined empirically or physically to delineate features in the data. Good delineation of features in the electron data can be accomplished choosing values on a physical basis.

An altitude of 100 km was chosen to examine the electron data because this altitude is normally associated with the calculation of the electron loss cone. The parameters V and V_ℓ were determined by Mizera and Fennell (1977) by examining the energy flux spectra of electrons and positive ions at pitch angles near 0^o and 180^o respectively. A circle rather than an ellipse best conforms to the data in Figure 1b, implying that $B_o/B \ll 1$. The zero potential point, then, is a considerable distance above the satellite. The equatorial value of magnetic field strength for the field line has been chosen for B_o. The values of electric potential and magnetic field strength, consistent with the model of Chiu and Schulz (1978), are V_ℓ = 3000 volts, V = 1000 volts, B_o = 20 gamma, B = .058 gauss and B_ℓ = .579 gauss. These parameters are used in equations (2) and (3) to calculate the solid curves shown in Figure 1.

One is struck immediately by the differences in character of the particle populations in the different regions of Figure 1b. In particular, the shape of the electron contour f = 10 sec^3-km^{-6} (the contour labeled I) follows the boundaries corresponding to region T in Figure 2b very well. The presence of a significant population of trapped particles suggests an electric field whose lifetime is long compared to the bounce time of the electrons. Within the context of the present model, region T is inaccessible to charged particles by adiabatic processes. Whipple (1977) has suggested that population might occur during the formation of the parallel electric field.

It is interesting to note that the f = 10 sec^3-km^{-6} electron contour follows a maximum in the velocity distribution function at a radius corresponding to 1 keV ($v = 1.87 \times 10^4$ km/sec) in the precipitating loss cone along the $+v_\parallel$ axis. When viewed in terms of precipitating flux, this ridge is seen as a peak in the energy flux spectrum at the acceleration potential, as predicted by Evans (1974) and shown in Figure 3 of Mizera and Fennell (1977). Inside the 1 keV circle on the upper half of Figure 1b, there is a relative minimum centered at approximately $v_\parallel = 1.1 \times 10^4$ km/sec, $v_\perp = 0$ in the region corresponding to S, I in Figure 2b along the $+v_\parallel$ axis. The electrons represented by the contours surrounding this minimum are of local ionospheric origin and have been reflected downward by the electric field above the satellite. Contours with the same values of f(v) can be seen along the $-v_\parallel$ axis in the region corresponding to S, I in Figure 2b. These contours, representing secondary electrons produced in the atmosphere, merge with the loss cone and are not closed. The electron population of magnetospheric origin, corresponding to region M in Figure 2b, is represented in Figure 1b by a series of concentric circles (isotropic except in the local loss cone) with a steep gradient. The electron populations are very well delineated by application of the theory of adiabatic

motion, a choice of potentials inferred from the data and selection of 100 km as the lower extent of adiabatic motion.

The positive ion data, determined to be predominately protons (Mizera and Fennell, 1977), are displayed in Figure 1a and is interpreted by means of an analysis similar to that used to interpret the electron data. The contours can be separated into a component roughly circular about the origin (v=0) and a component circular about a velocity corresponding to an energy of 1.4 keV ($v_{\parallel} = -5.2 \times 10^2$ km/sec). The latter represents an ion beam coming out of the ionosphere. Delineation of the features exhibited in the ion contours in Figure 1a cannot be accomplished by a simple choice of magnetic field and electric potential parameters in equation (2). Parameters associated with two altitudes which have a physical significance have been used to define boundaries with which to examine the ion data; altitude 100 km, which is important in determining the electron loss cone, and altitude 2000 km, which is important when considering proton charge exchange interactions as discussed below. Also, the parameters of a hyperbola which does separate the ion beam from its surroundings is examined for possible physical significance. Although definite conclusions are not drawn from the ion data, examination of the data with respect to the several curves presented does provide a perspective. The curve labeled 100 km in Figure 1a corresponds to the atmospheric loss cone as defined by equation (2) using the same parameters as in the electron data. It is apparent that the criterion defining the loss cone for electrons does not define the source region for positive ions. The shape of the ion beam contours in the $-v_{\parallel}$ direction suggests that the ions are being accelerated from source points located over a range of altitudes along the magnetic field line above 100 km. Chiu and Schulz (1978), using the CIRA (1972) model of the

neutral atmosphere, have estimated the altitude below which charge exchange becomes an important loss mechanism for magnetospheric protons (and above which protons are relatively free of charge exchange collisions over a full bounce period) to be 2000 km.

It is interesting to look at the ion data in relation to the boundary determined by positive ions which mirror at 2000 km. The electric potential representative of the 2000 km altitude on this magnetic field line is determined by arbitrarily assuming a linear potential as a function of altitude between the satellite and 100 km altitude. The hyperbola labeled 2000 km in Figure 1a is the result of using V_ℓ = 2470 volts and B_ℓ = 0.263 gauss in equation (2).

In this case the $-v_\parallel$ intercept of the 2000 km curve approximates the apparent center of the concentric ion beam contours. In this sense the latter curve is the best estimate of the source region. That is, the region which corresponds to I in Figure 2a, representing particles of ionospheric origin, lies in the altitude region from which hot magnetospheric protons are lost due to charge exchange. The electron data alone cannot be used to resolve the potential below the satellite sufficiently to determine whether the potential at 100 km is 3000 volts or 2500 volts. Both values produce equally satisfying boundaries to region T. The inability to accurately determine the loss cone boundary given by equation (2) is due to the fact that $|(B_\ell/B)-1| \approx 9$, requiring a large change in $(V_\ell - V)$ to produce a detectable change in the $v_\perp$ intercept (ref. Figure 2b). The implication derived from the ion data is that a potential of (approximately) 2500 volts is reasonable for a source altitude of 2000 km. Consequently below 2000 km neither the electron data nor the collisionless quasi-neutral equilibrium model of Chiu and Schulz (1978) are definitive.

The ion contours, in the $-v_{\parallel}$ half plane of Figure 1a, exhibit several points where the contours change direction abruptly. On the $-v_{\parallel}$ axis there is a natural location ($-v_{\parallel}$ = 180 km/sec) for the intercept of the hyperbola, which determines the value of the electric potential to be used. A hyperbola approximating these points can be obtained, using V_{ℓ} = 1170 volts and B_{ℓ} = .137 gauss (the 4000-km dipole field value), which might be interpreted as the boundary between magnetospheric and ionospheric ions. This hyperbola is shown in Figure 1a labeled 4000 km. Although this curve has been determined empirically, the electric potential used is not an unreasonable physical possibility.

This empirically determined curve suggests that the ion source is extended above 100 km and may be significant at much higher altitudes and that the model used by Chiu and Schulz (1978) requires refinement. Chiu (private communication, 1977) has suggested that the particles in the ion beam originating in the ionosphere experience charge exchange collisions as they are accelerated up the magnetic field line. The low energy ion resulting from a charge exchange collision is accelerated up the field line through only a fraction of the potential difference between the satellite and the ionosphere, depending on the location of the collision. The result gives the appearance of an extended source. Considering the simplicity of the model used by Chiu and Schulz (1978), it is not surprising that an exact boundary between ionospheric and magnetospheric ions is difficult to determine.

In summary, the effects of an electric field parallel to the earth's dipolar magnetic field in the auroral region has been discerned by organizing the charged particle data into contours of constant velocity-space distribution function. Particle data taken on August 12, 1976, by the S3-3 satellite have provided evidence of a parallel electric field with a potential drop of 1000 volts above the satellite and 2000 volts below the satellite. The

observed particle populations are separated in velocity-space by recognizable demarcations calculated from the conservation laws (which include the electric potential) in accordance with Liouville's theorem. It is clear that the high temporal and spatial resolution of charged particle data displayed in these velocity-space representations is a crucial tool for studying particle dynamics in auroral particle research.

REFERENCES

Chiu, Y. T., and M. Schulz, Self-consistent particle and parallel electrostatic field distributions in the magnetosphere-ionospheric auroral region, J. Geophys. Res., to be published, 1978.

Evans, D. S., Precipitating electron fluxes formed by a magnetic field aligned potential difference, J. Geophys. Res., 79, 2853, 1974.

Mizera, P. F., and J. F. Fennell, Signatures of electric fields from high and low altitude particle distributions, Geophys. Res. Letters, 4, 311, 1977.

Whipple, E. C., Jr., The signature of parallel electric fields in a collisionless plasma, J. Geophys. Res., 82, 1525, 1977.

THE IVAN A. GETTING LABORATORIES

The Laboratory Operations of The Aerospace Corporation is conducting experimental and theoretical investigations necessary for the evaluation and application of scientific advances to new military concepts and systems. Versatility and flexibility have been developed to a high degree by the laboratory personnel in dealing with the many problems encountered in the nation's rapidly developing space and missile systems. Expertise in the latest scientific developmentc is vital to the accomplishment of tasks related to these problems. The laboratories that contribute to this research are:

Aerophysics Laboratory: Launch and reentry aerodynamics, heat transfer, reentry physics, chemical kinetics, structural mechanics, flight dynamics, atmospheric pollution, and high-power gas lasers.

Chemistry and Physics Laboratory: Atmospheric reactions and atmospheric optics, chemical reactions in polluted atmospheres, chemical reactions of excited species in rocket plumes, chemical thermodynamics, plasma and laser-induced reactions, laser chemistry, propulsion chemistry, space vacuum and radiation effects on materials, lubrication and surface phenomena, photosensitive materials and sensors, high precision laser ranging, and the application of physics and chemistry to problems of law enforcement and biomedicine.

Electronics Research Laboratory: Electromagnetic theory, devices, and propagation phenomena, including plasma electromagnetics; quantum electronics, lasers, and electro-optics; communication sciences, applied electronics, semiconducting, superconducting, and crystal device physics, optical and acoustical imaging; atmospheric pollution; millimeter wave and far-infrared technology.

Materials Sciences Laboratory: Development of new materials; metal matrix composites and new forms of carbon; test and evaluation of graphite and ceramics in reentry; spacecraft materials and electronic components in nuclear weapons environment; application of fracture mechanics to stress corrosion and fatigue-induced fractures in structural metals.

Space Sciences Laboratory: Atmospheric and ionospheric physics, radiation from the atmosphere, density and composition of the atmosphere, aurorae and airglow; magnetospheric physics, cosmic rays, generation and propagation of plasma waves in the magnetosphere; solar physics, studies of solar magnetic fields; space astronomy, x-ray astronomy; the effects of nuclear explosions, magnetic storms, and solar activity on the earth's atmosphere, ionosphere, and magnetosphere; the effects of optical, electromagnetic, and particulate radiations in space on space systems.

THE AEROSPACE CORPORATION
El Segundo, California

• • •